NATURAL CONVECTION BETWEEN A PAIR OF ELLIPTICAL CYLINDERS IN BLUNT AND SLENDER SITUATIONS

الحمل الحراري الطبيعي بين زوج من الأسطوانات الأهليليجية فى وضع كليل وآخر رشيق

El-Desouki Ibrahim Eid

Associate Prof., Mech. Dept., Faculty of Industrial Education, Suez Canal University, 43515 Suez, Egypt.

ملخص

فـــي هـــذا الـــبحث يتم دراسة انتقال الحرارة بالحمل الطبيعى بين زوج من الأسطوانات الإهليليجية لهما نسب أهليل متغيرة فى وضع كليل وآخر رشيق عمليا وعدديا. تم تصنيع ثلاثة أزواج من الأسطوانات الإهليليجية لهم نفس نسبة القطـــر الخارجـــى الـــى القطر الداخلى ولهم نسب أهليل ٠,٦٦٢، ٠,٨٦٦، ٠,٩٦٨ باستخدام ماكينة القطع السلكى المبـــرمجة باســـتخدام الحاسب الآلي. أجريت الأختبارات المعملية عن طريق الحفاظ على فيض حرارى ثابت على ســـطح الأســـطوانة الداخلية وتبريد سطح الأسطوانة الخارجية. تم دراسة تأثير اللامركزية الرأسية الموجبة والسالبة واللامركزية الأفقية وزواية التصدى للأسطوانة الداخلية على الحمل الحرارى الطبيعى بين كل زوج من الأسطوانات الإهليليجـــية علـــى حد سواء فى الوضع الكليل والوضع الرشيق. تم الربط بين النتائج المعملية بمعادلة تجريبية ذات نـــسبة خطـــأ مقبولة. تمت محاكاة حالة الدراسة عدديا باستخدام برنامج معد خصيصا للحل العددي لديناميكا الموائع CFD لتوضـــيح نمط التدفق والسلوك الحراري للهواء داخل الفراغ الإهليليجي الحلقى بين كل زوج من الأسطوانات الإهليليجـــية. فـــي ضوء مقارنة بعض نتائج البحث الحالي مع نظائرها من البحوث السابقة تبين وجود توافق بينهم. وفـــي ضوء مقارنة نتائج البحث الحالي تبين أن اللامركزية الرأسية تعزز الحمل الحرارى الطبيعى فى حدود ١٥% وأن اللامركـــزية الأفقـــية تعزز الحمل الحرارى الطبيعى فى حدود ١٠% والوضع الرشيق لزوج من الأسطوانات الإهليليجية يعزز الحمل الحرارى الطبيعى بنسبة تتراوح بين ٣٠% - ٤٠% عن الوضع الكليل.

ABSTRACT

In this paper, natural convection heat transfer between pairs of elliptical cylinders having different elliptical ratios in blunt and slender situations was studied experimentally and numerically. Three pairs of elliptical cylinders having the same axes ratio of 2 and elliptical ratios of 0.662, 0.866 and 0.968 were cut using CNC wire-cut machining. The tests were carried out by keeping the inner cylinder at a constant heat flux while cooling the outer one. The effects of vertical eccentricity, horizontal eccentricity and angle of attack of the inner cylinder on natural convection for both blunt and slender situations of each pair were stated. Empirical correlation was deduced within acceptable uncertainty for the experimental results. A validated numerical CFD model was conducted with the case study to clarify the thermal behavior of air inside the elliptical annulus space between the two elliptical cylinders. Compatible and satisfactory to the conscience agreement was found in the comparison among present and corresponding previous works. In the vision of the comparison among the results of present work, it was found that the vertical eccentricity can enhance natural convection by about 15% than the concentric case, the horizontal eccentricity can enhance natural convection by about 10% than concentric case and slender situation leads to about 30% - 40% enhancement in natural convection than the blunt situation for the same elliptical ratio.

Keywords: Elliptical cylinders, blunt, slender, eccentric, angle of attack and CFD modeling.

NOMENCLATURE

a	Semi-major axis, m	g	Gravity acceleration, m/s^2
b	Semi- minor axis, m	h	Convective heat transfer coef., $W/m^2.K$
C	Specific heat, $J/kg.K$	**h**	Average heat transfer coef., $W/m^2.K$
Gr	Grashof number		
F	Shape factor		

Accepted December 1, 2009.

i	Electric current, *Ampere*
k	Thermal conductivity, $W/m.K$
L	Cylinder length, m
Nu	Local Nusselt number
Nu	Average Nusselt number
Pr	Prandtl number
P	Pressure, N/m^2.
Q	Heat transfer rate, W
q	Heat flux, W/m^2
Ra	Rayleigh number
r	Radius, m
T	Temperature, K
t	Cylinder wall thickness, m
v	Voltage, *volt*
u	Velocity vector, $= u\bar{i} + v\bar{j} + w\bar{k}$, m/s
u, v, w	Velocity components, m/s
x, y, z	Cartesian coordinates, m
α	Thermal diffusivity, m^2/s
β	Coefficient of volume expansion, K^{-1}
δ	Eccentricity, m
ε	Surface emissivity,
ϕ	Angle of attack, *degree*
λ	Characteristic length, m $= a_o - a_i$ for slender; $= b_o - b_i$ for blunt.
υ	Kinematic viscosity, m^2/s
μ	Dynamic viscosity, $kg/m.s$
ρ	Density, kg/m^3
σ	Stefan-Boltzmann const., W/m^2K^4
ξ	Elliptical ratio

Subscripts

a	Air
c	Mid-length section
e	End-section
h	Horizontal
i	Inner cylinder
o	Outer cylinder
s	Solid
v	Vertical

INTRODUCTION

The natural convection heat transfer between circular or elliptical cylinders becomes important in recent decade due to its numerous associations with electrical transmission lines, solar collectors-receivers, insulations and flooding protection for buried pipes used for district heating and cooling, nuclear reactors, space heating, refrigerator condensers, heating of oils for ease of pumping, heat exchangers, passive solar energy collectors, geothermal systems, crude oil production, electronics cooling, fiber and granular insulations, solidification of castings, and many of machining processes. Many of recent investigations for natural convection in the eccentric annular spaces have been performed. Numerical solution was done for natural convection heat transfer from an elliptic heat source buried beneath porous medium by Facas [1]. The results were presented for $10 \le Ra \le 200$ and $0.167 \le b/a \le 1.0$. The slender orientation of the elliptic heat source yields much higher heat transfer rates at low b/a than the blunt orientation. A numerical study for natural convection heat transfer between two isothermal eccentric horizontal cylinders was done by Raghavarao et. al. [2]. The solution was obtained for $10^3 \le Ra \le 10^5$, Pr=12 and axes ratios of 1.0 and 2.0. It was found that the minimum heat transfer is observed when the two cylinders are concentric. The DQ (differential quadrate method) was employed to divide the derivatives in the governing equations of the natural convection between eccentric inner circular cylinder and outer square cylinder by Shu et. al. [3]. This study considered $Ra = 3\times10^5$ and a cylinder length $L = 2.2r_i$. The validated DQ method found out that the eccentricity has significant effects on plume inclination. The influence of Prandtl numbers on the natural convection between vertically eccentric cylinders was studied numerically by Projahn et. al. [4].

The study considered $10^3 \le Ra \le 10^5$, $0.7 \le Pr \le 100$ and $\delta / \lambda = \pm 0.625$. The results were correlated by using a regression analysis within 3% uncertainty. The natural convection from a horizontal cylinder in a rectangular cavity was investigated numerically and experimentally by Cesini et. al. [5]. The study considered $1.3\times10^3 \le Ra \le 7.5\times10^4$, air is the working fluid and the ratio of the cavity width was changed from $4.2r_i$ to $8.6r_i$. It was found that the increase in Rayleigh number with decreasing the cavity width leads to an increase in heat transfer rate. Laminar free convection heat transfer from a vertical array of horizontal elliptic cylinders with vertical major axis had been experimentally investigated by Yousefi et. al. [6]. The spacing between two successive cylinders was changed from $2a$ to $5a$. Correlations were developed for both an individual cylinder in the array and the whole array for $10^3 \le Ra \le 2.5\times10^3$. It was found that the heat transfer increased by increasing cylinder spacing. Experimental and numerical studies for natural convection from concentric elliptical cylinder to a large circular cylinder were carried out by Sakr et. al. [7]. Experimental work scanned $1.12\times10^7 \le Ra \le 4.9\times10^7$ and a rotation angle from 0^0 to 90^0 with b/a=0.333. The numerical study covered $0.1 \le b/a \le 0.98$ and a hydraulic radius ratio from 1.5 to 6.4. It was found that Nusselt number increases with the rotation angle. Also, Nusselt number decreases with the radius ratio up to 1.75 then it increases for higher radius ratios. The effect of attack angle on natural convection from a horizontal elliptic tube having b/a=0.5 was investigated experimentally by Elshazly et. al. [8]. The angle of attack was varied from 0^0 to 90^0. The experiments covered $1.45\times10^6 \le Ra \le 1.78\times10^7$. It was found that local Nusselt number increases with the increase of attack angle. The natural convection from an isothermal horizontal elliptical cylinder with b/a=0.5 and 0.75 in two fluids having Pr=1 as well as 3 was studied analytically for slender and blunt orientations by Cheng [9]. It was found that the heat transfer rate for slender orientation is higher than that of blunt orientation. Natural convection from a horizontal square cylinder inside a vertical adiabatic channel was studied using finite difference method by Khodary et. al. [10]. The solution was obtained for square side length to channel width aspect ratio from 0.1 to 0.8. The cylinder was placed at mid-height of the channel at different lateral locations. The results determined the optimum aspect ratio over a range of Grashof number $1.0 \le Gr \le 3\times10^6$. An experimental study of natural convection between a circular cylinder envelope and an internal concentric heated square cylinder with two slots was performed by Li et. al. [11]. The internal cylinder was a hollow one with two horizontal slots up and down. The ratio of the slot width to the square side length was taken 0.0612 for $1.77\times10^2 \le Ra \le 8.72\times10^6$ and 0.3878 for $1.32\times10^2 \le Ra \le 6.25\times10^6$. It was found that the two slots can enhance the heat transfer by about 31% and 54.2% respectively. The distribution of the surface heat transfer from two horizontal heated cylinders under natural convection conditions in water was found out experimentally by Reymond et. al. [12]. The study considered $Ra = 2\times10^6$, 4×10^6 and 6×10^6 with a spacing of 1, 2 and 3 times of the cylinder diameter. The measurements were taken with heating of both cylinders, heating the upper cylinder only or heating the lower cylinder alone. It was shown that the plume rising from the lower heated cylinder interacts with the natural convective flow around the upper heated cylinder. It enhances the turbulent mixing and consequently the natural convective heat transfer. Natural convection from a heated horizontal cylinder has been investigated experimentally by Atmane et. al. [13] in

water with the free surface either closes to the cylinder surface or raises the cylinder surface by a depth from fifth to three times of the cylinder diameter. It was noticed that the natural convection flow around the cylinder can undergo a transition from stable to unstable when the depth of the cylinder bellow the free surface equals roughly the diameter of the cylinder.

Upon the previous review and up to author knowledge, there is a shortage in studying the effects of the curricular parameters that strongly affecting natural convection between two elliptical cylinders. These parameters are the elliptical ratio with keeping the surface area to be the same, vertical eccentricity, lateral eccentricity, blunt orientation, slender orientation and angle of attack. Upon this vision, three pairs of elliptical cylinders having the same corresponding surface area were cut using CNC wire-cut machining and they were experimentally tested to scan the effects of the previous parameters. Also, a validated CFD modeling was conducted with the case study to give a full concept of the problem. The experimental results could be interpreted upon the CFD images.

EXPERIMENTAL WORK

Test specimens

The ellipse is a planer *x-y* curve where the loci of its all points satisfy:

$$x^2/a^2 + y^2/b^2 = 1 \qquad (1)$$

It has an elliptical ratio:

$$\xi = \sqrt{1-(b^2/a^2)} \qquad (2)$$

Three pairs of elliptical cylinders having an equal axes ratio of 2, an equal length of 0.9 *m* and an equal corresponding surface area were cut from aluminum by using the wire-cut JSEDM machining, [14]. Each pair has the following tabulated dimensions, table (1):

Table (1), Main dimensions of the three tested specimens.

Pair No.	a_i, *mm*	b_i, *mm*	a_o, *mm*	b_o, *mm*	$\xi = \sqrt{1-(b^2/a^2)}$
1	57.15	42.85	114.30	85.70	0.662
2	66.67	33.33	133.33	66.67	0.866
3	80.00	20.00	160.00	40.00	0.968

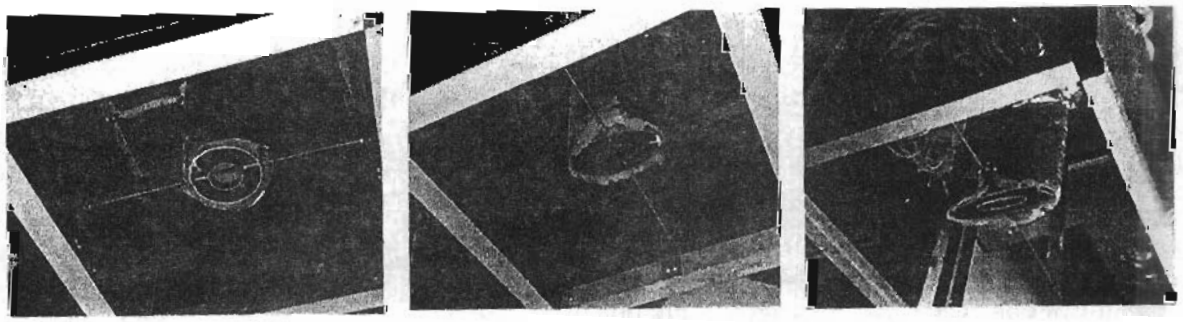

Pair No. 1 Pair No. 2 Pair No. 3

Figure (1), Photographs of the three tested pairs.

Apparatus

The experimental apparatus, shown in figure (2), contains mainly one pair of the tested specimens (1 and 2), a heater (3), a voltmeter, an ammeter, an auto-transformer (4), twenty four thermocouples (7), suspension wires (10), two-vertical threaded bars (11), two-horizontal threaded bars (12), tilting mechanism with a protractor (14 and 15), and a temperature

indicator. Each pair of the specimens were oriented horizontally either blunt (major axis is horizontal) or slender (major axis is vertical). The two vertical threaded bars were used to adjust the vertical eccentricity and the two horizontal ones were used to adjust the lateral eccentricity. A tilting mechanism with a protractor was used to rotate the inner cylinder in an increment of 15^o, without rotating the outer cylinder. The inner elliptical cylinder was heated by a nickel-chrome electric heater. Ten *K-type* thermocouples were used to measure the temperatures of the outer surface of the inner cylinder, [15]. They were situated on five sections; two thermocouples are on each section with 180^o between them with a revolving angle of 72^o between two successive sections. Another ten thermocouples were used to measure the temperature of the inner surface of the outer cylinder. Three thermocouples were used to measure the air temperature inside the gap between the cylinders. One thermocouple measures the room temperature of the closed laboratory. A digital temperature indicator of $0.1\,^oC$ resolution was used to record the temperatures. The power consumed by the heater was measured by an ammeter of 0.01 *Ampere* resolution and a voltmeter of 0.1 *volt* resolution.

Experimental uncertainty analysis

The uncertainty of the measured results is caused by random and systematic errors in the measurements, it consists mainly of;

Uncertainty of electric current, $\Delta i = 0.1$ *Ampere*

Uncertainty of voltage, $\Delta v = 0.1$ *volt.*

Uncertainty of temperature, $\Delta T = 0.1^oC$.

Uncertainty of eccentric distance, $\Delta\delta = 0.01$ *mm.*

Uncertainty of angle of attack, $\Delta\phi = 1^o$.

Generally, the uncertainty of the present measurement lies within the range 2.5% to 4%.

Experimental program

Referring to figure (3), each pair was tested alone for orientation cases from (a) to (h). Thus; the range and the parameters to be studied are as follows:

Elliptical ratio; $0.662 \le \xi \le 0.968$

Vertical eccentricity; $-0.5 \le \delta_v / \lambda \le +0.5$

Horizontal eccentricity; $0.0 \le \delta_h / \lambda \le +0.5$

Angle of attack;

$0.0^o \le \phi \le 90^o$ for pair No. 1.

$0.0^o \le \phi \le 45^o$ for pair No. 2.

$0.0^o \le \phi \le 15^o$ for pair No. 3.

Experimental data reduction

The heat transfer by natural convection between inner and outer elliptical cylinders is, [16]:

$$Q_{convection} = v\,i - Q_{radiation} - Q_{conduction} \quad (3)$$

$$Q_{radiation} = \left(\pi\sigma(a_i + b_i),\, L\, \varepsilon_i\, (T_i^4 - T_o^4)\right) + \left(\frac{F_{i-o}\ \pi\sigma\ (a_i + b_i)\ L\ (T_i^4 - T_o^4)}{1/\varepsilon_i + ((1-\varepsilon_o)/\varepsilon_o)\ ((a_i + b_i)/(a_o + b_o))}\right) \quad (4)$$

$$Q_{conduction} = \frac{2\,\pi(a_i + b_i)\,t\,(T_c - T_e)}{L/2k_s} \quad (5)$$

The average convective heat transfer coefficient, average Nusselt number and Rayliegh number are calculated as follows:

$$\mathbf{h} = Q_{convection} / \left[\pi(a_i + b_i) L\ (T_i - T_o)\right] \quad (6)$$

$$\mathbf{Nu} = \mathbf{h}\,\lambda / k \quad (7)$$

$$Ra = \frac{g\ \beta\ (T_i - T_o)\ \lambda^3}{\upsilon^2}\ Pr \quad (8)$$

The air properties in the above equations were determined at an average temperature, T, [17], [$\mathbf{T} = (T_i + T_o)/2$].

NUMERICAL MODEL

The flow of the case study investigated herein is considered to be three dimensional, steady, laminar and incompressible except for Boussinesq approximation for density in the buoyancy term in *y*-momentum equation. So the governing equations could be reduced as follows; [18 and 19] to:

Continuity equation; $div\ (\rho\ u) = 0$ (9)

Momentum equations;

$$div(\rho u\ \mathbf{u}) = -\partial p/\partial x + div\ (\mu\ grad\ u) \quad (10)$$

$$div(\rho v\ \mathbf{u}) = -\partial p/\partial y + div(\mu\ grad\ v) + \rho_\infty g\,\beta(T - T_\infty) \quad (11)$$

$$div(\rho w\ \mathbf{u}) = -\partial p/\partial z + div(\mu\ grad\ w) \quad (12)$$

Energy equation;

$$div(\rho C T\ \mathbf{u}) = div(k\ grad\ T)$$
$$\alpha \nabla^2 T = div\ (T) \quad (13)$$

The boundary conditions are:

- At the surface of inner elliptical cylinder;

$$u = v = w = 0, \quad q' = const. \quad (14)$$

- At the surface of the outer elliptical cylinder;

$$u = v = w = 0; \quad T = T_\infty \quad (15)$$

- At the symmetry plane; $x = 0.0$

$$\partial u/\partial x = \partial v/\partial x = \partial w/\partial x = \partial p/\partial x = \partial T/\partial x = 0 \quad (16)$$

The volume between the inner and outer elliptical cylinders was drawn in Gambit such as x-axis is the semi-major axis; y-axis is the semi-minor one and z-axis is the meridian center of the volume. A quad-pave meshing was applied to the elliptical annuli face of the volume and hence a hexagonal cooper meshing was applied for the volume. The boundary conditions on the surfaces of both inner and outer elliptical cylinders were identified, insulation walls were also defined, solid and fluid volumes were also specified. The Gambit model was exported to the 3-D Fluent solver. A 3-D implicit steady solver was selected and the gravity effect was considered in the negative direction of y-axis. The thermal properties of air were assumed to be changed versus its temperature as a piece-wise linear. The values of the heat flux and the temperature were fed as boundary conditions. The solver solves numerically the governing equations using SIMPLE first order upwind scheme to do several iterations until the solution converges at certain acceptable residuals, [20].

RESULTS AND DISCUSSION

Natural convection is arising as a result of up flow fluid motion due to density changes resulting from heating processes. The natural convection between a pair of elliptical cylinders having the same axes ratio with different elliptical ratios was studied herein. Figure 4 shows average Nusselt number against Rayleigh number for the pair No. 1 in different eccentricities for blunt situation. The figure shows that the heat transfer is converted from conduction regime to convection regime at $Ra \approx 3000$, which is a fair consistent with the data of Kumar et. al. [21]. Referring to figures (6 and 8), as the inner elliptical cylinder was kept at a constant heat flux which results in high temperature on its surface; the air near the inner surface rises upward due to the thermal expansion. The uprising plume is then cooled by the cold outer cylinder. The denser air is eventually dropped downward along the surface of the outer cylinder as shown in figure (7). As a consequence, non circular vortices will form in steady-state condition. The center of the stronger vortices is shifted upward while the center of weak ones is shifted downward as shown in figure (9). Positive and negative eccentricities between the two elliptical cylinders offer slightly increase in natural convection as shown in figure (4). This is due to the air temperature near the inner cylinder for eccentric cases are slightly higher than that of the concentric case as shown in figures (6 and 10). This will produce slightly stronger buoyancy driven upward plume, as shown in figures (7 and 11).

Figure (6) shows the CFD static temperature plot versus x-axis of the cross-section at the mid-length of the cylinders. It is clear that, for horizontal eccentricity to the right, the narrow right gap has hotter air than the left wide gap which produces narrow non-circular stronger vortices through the right gap than those through the left gap, as shown in figure (11). The hotter vortices in the right gap drive the up

flow plume which enhances the natural convection between the cylinders. Also, the rotation of inner cylinder while keeping the outer one without rotation will significantly enhance the natural convection between the two elliptical cylinders, as shown in figure (5). Referring to figures (and 12), the inner elliptical cylinder was rotated with an angle of attack ϕ, which causes the air near the top edge of the inner cylinder hotter than that at the bottom edge and as a consequence stronger vortices are formed at the top edge while weak vortices are formed at the bottom edge, as shown in figure (13).

The lower elliptical ratio for the pair No. 1 reduces the flow resistance for the up flow plume in blunt situation (concentric, vertically eccentric, horizontally eccentric and rotation with certain attack angle) if it is compared with higher elliptical ratios for pairs No. 2 and 3 as clear in figures (4, 14 and 15). However, in slender situation the higher elliptical ratio improves the natural convection between the two elliptical cylinders as shown in figures (16, 17 and 18).

Figure (19) shows that the positive vertical eccentricity results in a slight enhancement in natural convection than that the negative eccentricity. Also, the percentage enhancement is higher for slender situation than that for blunt situation. The same tendencies are even more accentuated in figure (20). The enhancement of natural convection is greatly affected by the angle of attack as clear in figure (21).

The experimental results were correlated as follows using the LAB FIT software within uncertainty of 11.16%.

$$\mathbf{Nu} = C \times Ra^{n} \times \xi^{m} \times \left[1 + \left|\frac{\delta_v}{\lambda}\right|^{a}\right] \times \left[1 + \left(\frac{\delta_h}{\lambda}\right)^{b}\right] \times \left[1 + c \times \sin\phi\right] \quad \text{for} \quad \begin{cases} 3\times10^{3} \le Ra \le 5.47\times10^{5} \\ 0.662 \le \xi \le 0.968 \\ -0.5 \le \delta_v/\lambda \le +0.5 \\ 0.0 \le \delta_h/\lambda \le +0.5 \\ 0.0^{o} \le \phi \le 90^{o} \quad \text{for } \xi=0.662 \\ 0.0^{o} \le \phi \le 45^{o} \quad \text{for } \xi=0.866 \\ 0.0^{o} \le \phi \le 15^{o} \quad \text{for } \xi=0.968 \end{cases} \tag{17}$$

Uncertainty = ± 11.16%

Orientation	C	n	m	a	b	c
Blunt	0.0566	0.3491	-0.1203	3.2102	4.2018	0.3809
Slender	0.0664	0.3815	1.2011	1.2010	2.8704	0.6841

COMPARISON BETWEEN PRESENT AND PREVIOUS WORKS

The comparison between present work and the previously published works in the literatures as well as the validation of the CFD model are shown in figure (22). As the characteristic length which is used in Nusselt number has various definitions in the literature works, the fair comparison has to be done using the convective heat transfer coefficient instead of Nusselt number.

Natural convection between vertically eccentric cylinders was studied numerically by Projahn et. al. [4] for $10^{3} \le Ra \le 10^{5}$, $0.7 \le Pr \le 100$ and $\delta_v/\lambda = \pm 0.625$. The results were correlated as follows within 3% uncertainty:

$$\mathbf{Nu/Nu}_{conduction} = 0.212 \times Ra^{0.243} \quad \text{for } \delta_v/\lambda = 0.0 \tag{18}$$

$$\mathbf{Nu/Nu}_{conduction} = 0.164 \times Ra^{0.264} \quad \text{for } \delta_v/\lambda = +0.625 \tag{19}$$

$$\mathbf{Nu/Nu_{conduction}} = 0.310 \times Ra^{0.214} \quad \text{for } \delta_v / \lambda = -0.625 \tag{20}$$

Experimental and numerical studies for natural convection from concentric elliptical cylinder to a circular cylinder were carried out by Sakr et. al. [7]. The results were correlated with a maximum error of ±10% as following:

$$\mathbf{Nu} = 1.264 \times Ra^{0.26}\ HRR^{0.35}\ (1+\sin\phi)^{0.301} \quad \text{for } 1.26\times10^4 \le Ra \le 5.6\times10^4,\ 0^\circ \le \phi \le 90^\circ \tag{21}$$

Figure (22) shows compatible and satisfactory to the conscience results as a good agreement is noted between CFD results and experimental data for the tested pair No. 1 when it is oriented as slender with $\phi = 60^\circ$. A fair matching between the present and previous works is also obtained.

CONCLUSIONS

In this work, natural convection heat transfer between pairs of elliptical cylinders having different elliptical ratios in blunt and slender situations was studied experimentally and numerically. The study scanned the effects of vertical eccentricity, horizontal eccentricity, angle of attack on natural convection of each pair. A 3-D CFD model was conducted with the present study to highlight the flow pattern of air inside the elliptical annular space between the two elliptical cylinders. The results of the study could be summarized in the following remarks:

1. Positive eccentricity can enhance the natural convection by about 15% than the concentric case and the enhancement ratio can increase with decreasing the elliptical ratio for blunt situation. Furthermore, positive eccentricity gives an enhancement ratio of about 40% than the concentric case and the ratio increases with decreasing the elliptical ratio in case of slender situation.
2. Horizontal eccentricity enhances the natural convection between elliptical cylinders by about 10% and the enhancement ratio increases with decreasing the elliptical ratio for both blunt and slender situations.
3. The rotation of the inner cylinder with an angle of attack leads to an enhancement in natural convection between the elliptical cylinders by about 50% and 70% if $\phi = 90^\circ$ for blunt and slender situations respectively.
4. CFD results are compatible with the experimental results that validate the CFD model to investigate other parameters that affect the natural convection between elliptical cylinders such as; axis ratio and other values of elliptical ratio.

REFERENCES

1. Facas, G.N., (1995), *Natural convection from a buried elliptic heat source*, Int. J. Heat and Fluid Flow, pp. 519-526.
2. Raghavarao, C.V. and Sanyasiraju, Y.V.S.S., (1996), *Natural convection heat transfer of cold water in an eccentric horizontal cylindrical annulus- a numerical study*, Computational Mechanics 18, pp.464-470.
3. Shu, C., Xue, H. and Zhu, Y.D., (2001), *Numerical study of natural convection in an eccentric annulus between a square outer cylinder and a circular inner cylinder using DQ method*, Int. J. of Heat and Mass Transfer 44, pp. 3321-3333.
4. Projahn, U. and Darmstadt, H.B., (1985), *Prandtl number effects on natural convection heat transfer in concentric and eccentric horizontal cylindrical annuli*, Wärme-und Stoffübertragung 19, pp. 249-254.
5. Cesini, G., Paroncini, M., Cortella, G. and Manzan, M., (1999), *Natural*

convection from a horizontal cylinder in a rectangular cavity, Int. J. of Heat and Mass Transfer 42, pp. 1801-1811.

6. Yousefi, T. and Ashjaee, M., (2007), *Experimental study of natural convection heat transfer from vertical array of isothermal horizontal elliptic cylinders*, Exp. Thermal and Fluid Science 32, pp. 240–248.
7. Sakr, R.Y., Berbish, N.S., Abd-Alaziz, A.A. and Hanafi, A.S. (2008), *Experimental and Numerical Investigations of Natural Convection Heat Transfer in horizontal Elliptic Annuli*, J. of Applied Sciences Research, 4(2), pp. 138-155.
8. Elshazly, K., Moawed, m., Ibrahim, E. and Emara, M., (2006), *Experimental investigation of natural convection inside horizontal elliptic tube with different angles of attack*, Energy Conversion and Management 47, pp. 35–45.
9. Cheng, C.Y., (2006), *The effect of temperature-dependent viscosity on the natural convection heat transfer from a horizontal isothermal cylinder of elliptic cross section*, Int. Communications in Heat and Mass Transfer 33, pp. 1021–1028.
10. Khodary, K. and Bhattacharyya, T.K., (2006), *Optimum natural convection from square cylinder in vertical channel*, Int. J. of Heat and Fluid Flow 27, pp. 167–180.
11. Li, H.Z., Li, W. and Tao, W.Q., (1995), *Experimental study of natural convection heat transfer between an outer horizontal cylindrical envelope and an inner concentric heated square cylinder with two slots*, Heat and Mass Transfer 30, Springer-Verlag, pp. 455-459.
12. Reymond, O., Murray, D. B. O'Donovan, T.S., (2008), *Natural convection heat transfer from two horizontal cylinders*, Exp. Thermal and Fluid Science 32, pp. 1702–1709.
13. Atmane, M.A., Chan, V.S.S., Murray, D.B., (2003), *Natural convection around a horizontal heated cylinder: The effects of vertical confinement*, Int. J. of Heat and Mass Transfer 46, pp. 3661–3672.
14. Jsedm, Wire Edm, Operation Instruction, Jiann Sheng Machinery & Electric Industrial Co., LTD.
15. Holman, J.P., (2001), *Experimental Methods for Engineers*, McGraw-Hill Int. Edition, Seventh Edition, New York, USA.
16. Holman, J.P., *Heat Transfer*, McGraw-Hill Co., Ninth Edition, New York, USA, (2002).
17. Cengel, Y. A. and Boles, M. A., (1998), *Thermodynamics: An Engineering Approach*, McGraw-Hill Co., Third Edition, NY. USA.
18. Faires, J.D and Burden, R., (1998), *Numerical Methods*, 2nd Edition, BROOKS/COLE PUBLISHING COMPANY, 511 Forest Lodge Road, Pacific Grove, CA 93950, USA.
19. Dubovsky, V., Ziskind, G., Druckman, S., Moshka, E., Weiss, Y. and Letan, R., (2001), *Natural Convection inside Ventilated Enclosure Heated by Downward-Facing Plate: Experiments and Numerical Simulations*, Int. J. of Heat and Mass Transfer, 44, pp 3155-3168.
20. FLUENT, Fluent user's guide, Lebanon, Fluent Inc., USA, (2000).
21. Kumar, R. and Keyhani, M., (1990), *Flow Visualization Studies of Natural Convective Flow in a Horizontal Cylindrical Annulus*, *Journal of Heat Transfer*, Vol. 112, pp. 784-787.

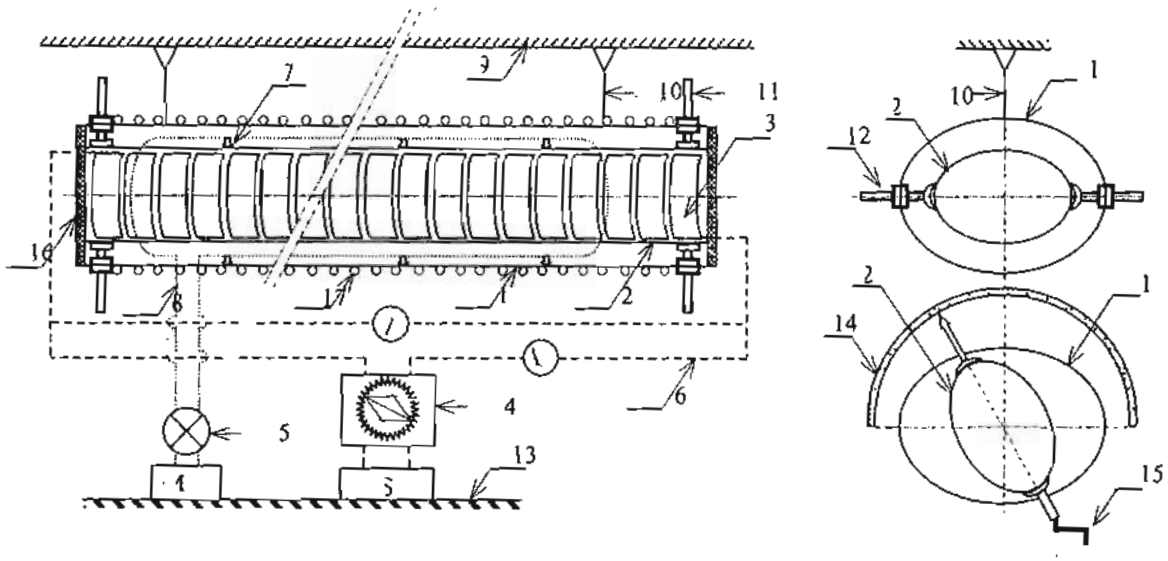

1- Outer elliptical cylinder
2- Inner elliptical cylinder
3- Electric Heater
4- Auto-transformer
5- Multi-switch (Selector)
6- Electric wire
A- Ammeter
7- Thermocouple
8- Thermocouple wire
9- Overhead ceiling
10- Suspension wire
11- Vertical threaded bar
12- Horizontal threaded bar
V- Voltmeter
13- Stand
14- Protractor
15- Handle
16- Wooden end plate
17- Cooling water coil
S- AC-supply
M- Temperature indicator

Figure (2), Experimental test-rig and measuring devices.

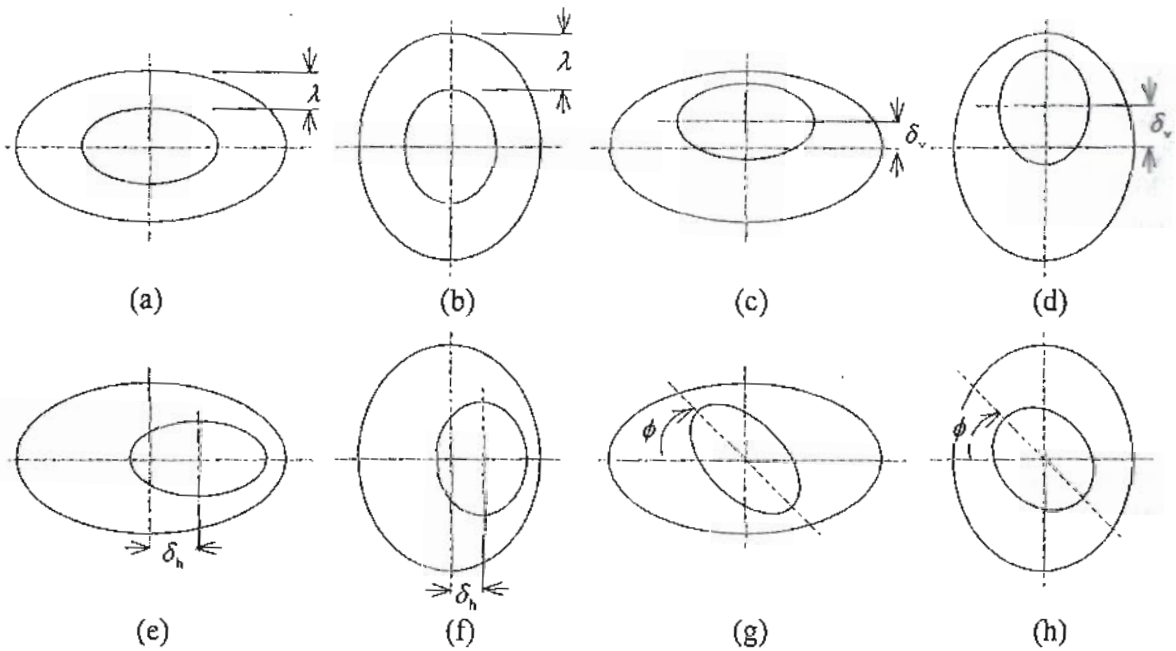

Figure (3), Schematic diagrams for blunt, slender, vertical eccentricity, horizontal eccentricity and angle of attack.

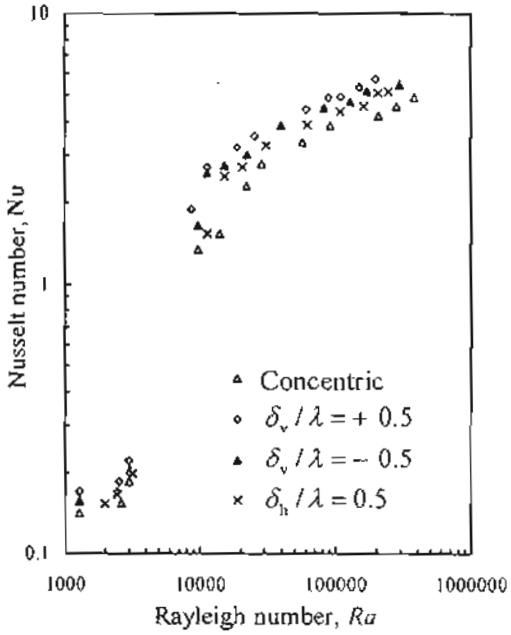

Figure (4), Nusselt number versus Rayleigh number for the pair No. 1 for different eccentricities in blunt situation.

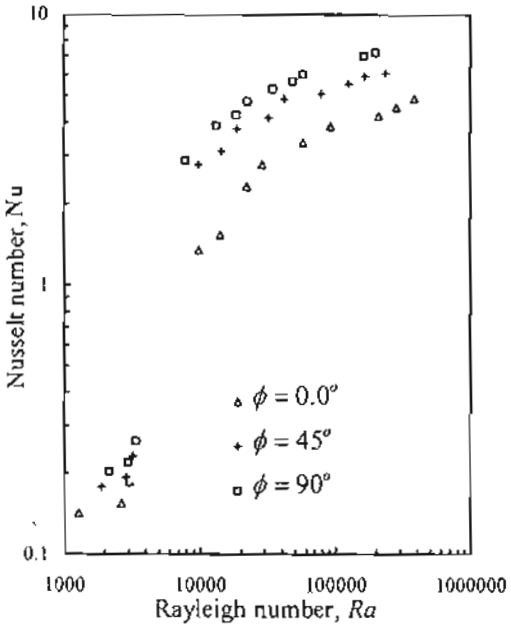

Figure (5), Nusselt number versus Rayleigh number for the pair No. 1 for different angle of attack in blunt situation.

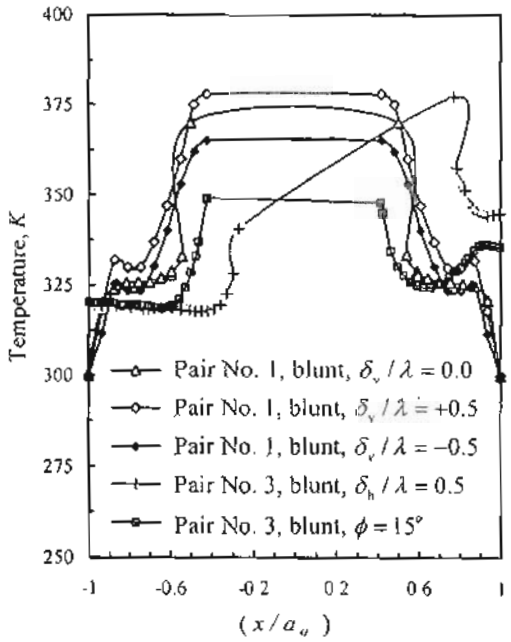

Figure (6), CFD temperature along x-axis of the cross-section at the mid-length of the pair No.1 and pair No.3 in blunt orientation for concentric, vertical eccentric and angle of attack situations.

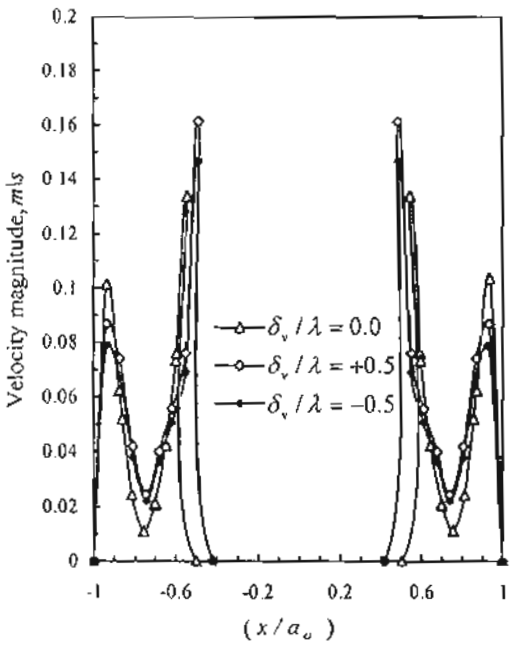

Figure (7), CFD velocity magnitude along x-axis of the cross-section at the mid-length of the pair No.1 in blunt orientation for concentric and vertical eccentric situations.

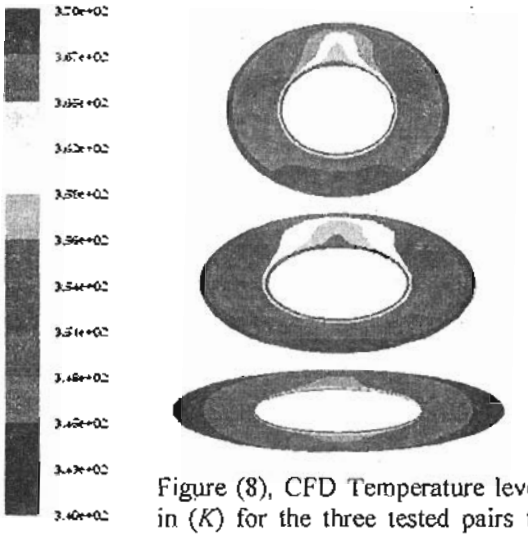

Figure (8), CFD Temperature levels in (K) for the three tested pairs for concentric and blunt orientation.

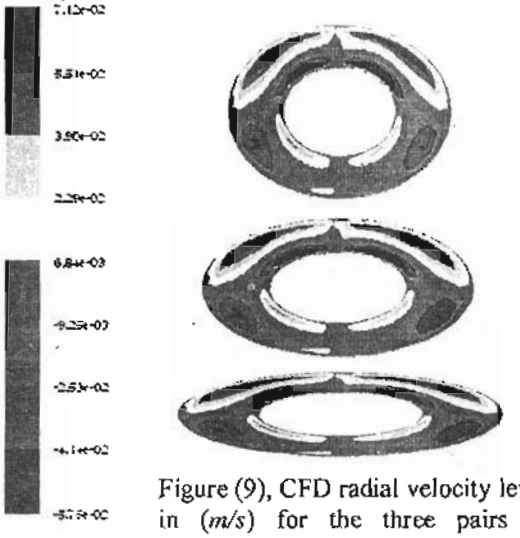

Figure (9), CFD radial velocity levels in (m/s) for the three pairs for concentric and blunt orientation.

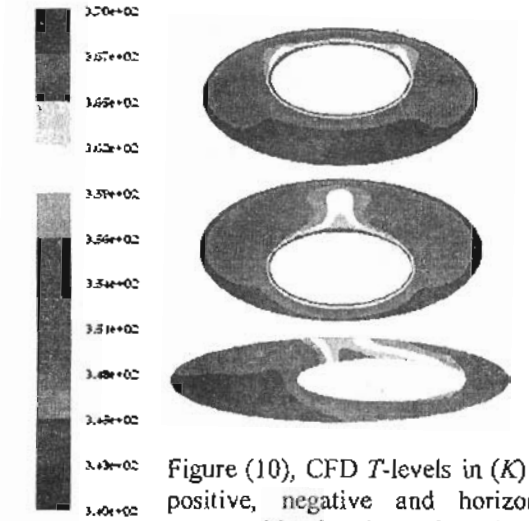

Figure (10), CFD T-levels in (K) for positive, negative and horizontal eccentricities for blunt orientation.

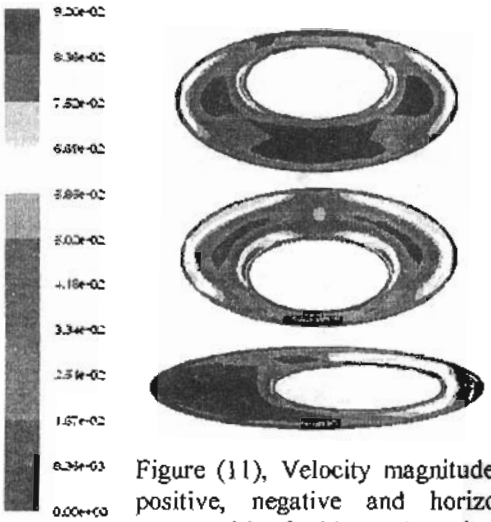

Figure (11), Velocity magnitude for positive, negative and horizontal eccentricities for blunt orientation.

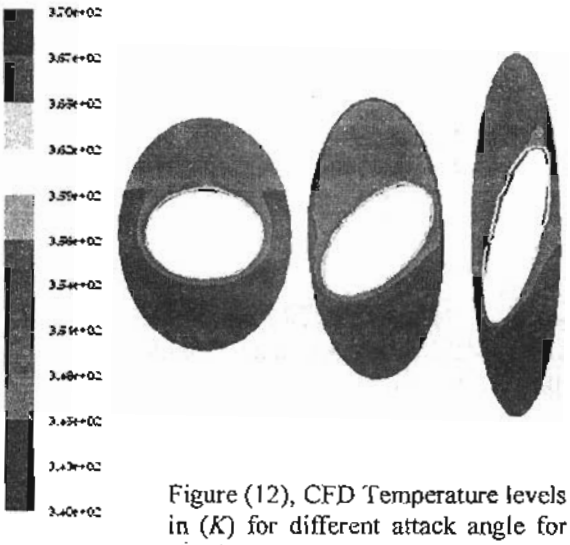

Figure (12), CFD Temperature levels in (K) for different attack angle for slender orientation.

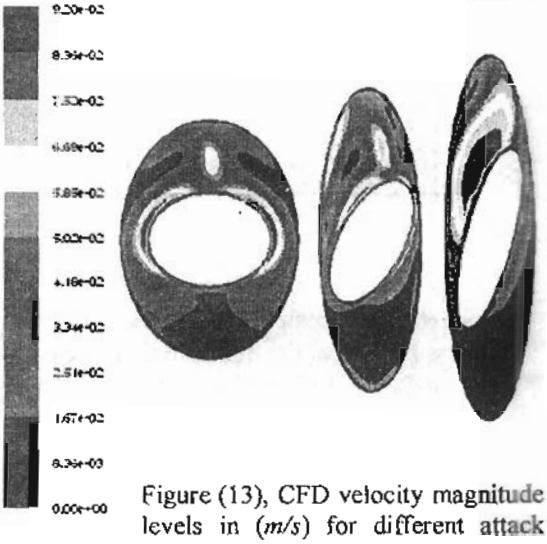

Figure (13), CFD velocity magnitude levels in (m/s) for different attack angle for slender orientation.

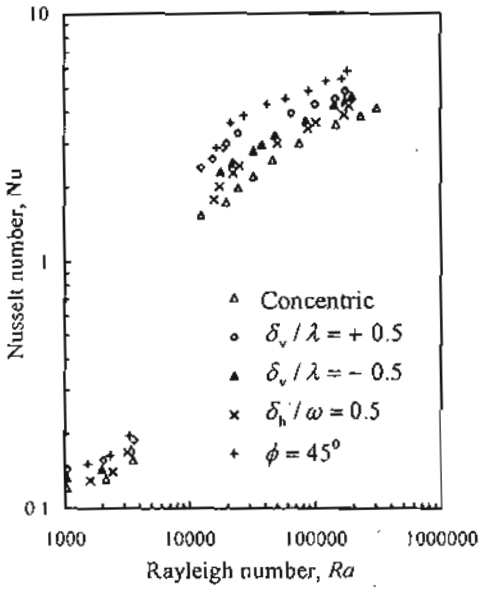

Figure (14), Nusselt number versus Rayleigh number for the pair No. 2 in different orientations for blunt situation.

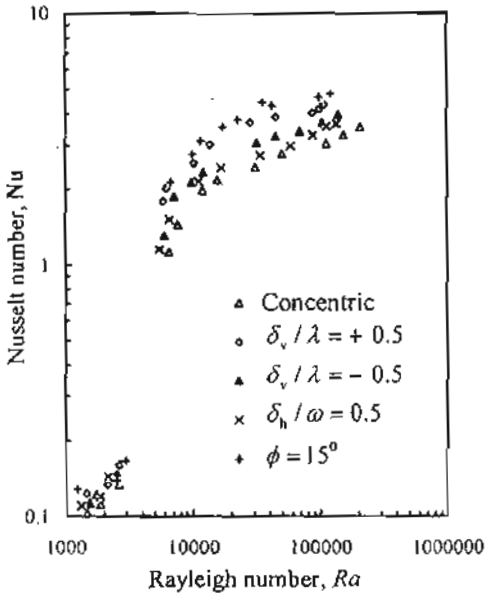

Figure (15), Nusselt number versus Rayleigh number for the pair No. 3 in different orientations for blunt situation.

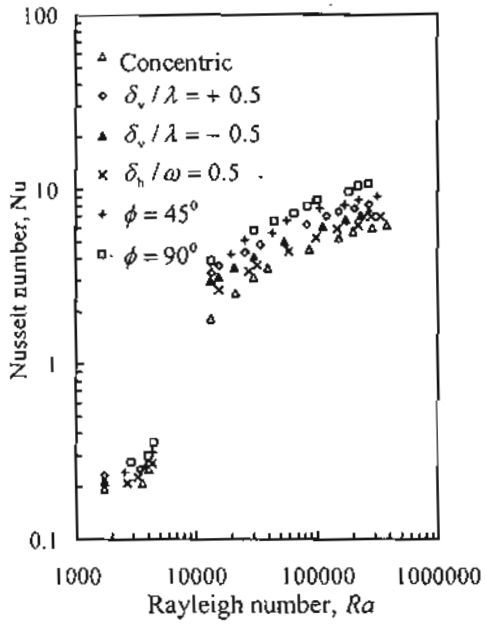

Figure (16), Nusselt number versus Rayleigh number for the pair No. 1 in different orientations for slender situation.

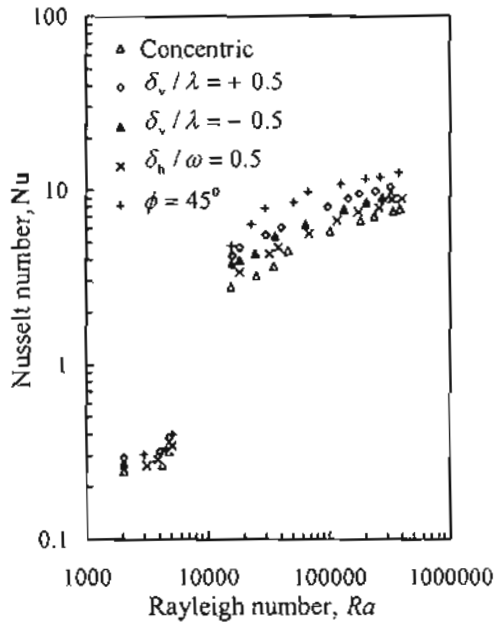

Figure (17), Nusselt number versus Rayleigh number for the pair No. 2 in different orientations for slender situation.

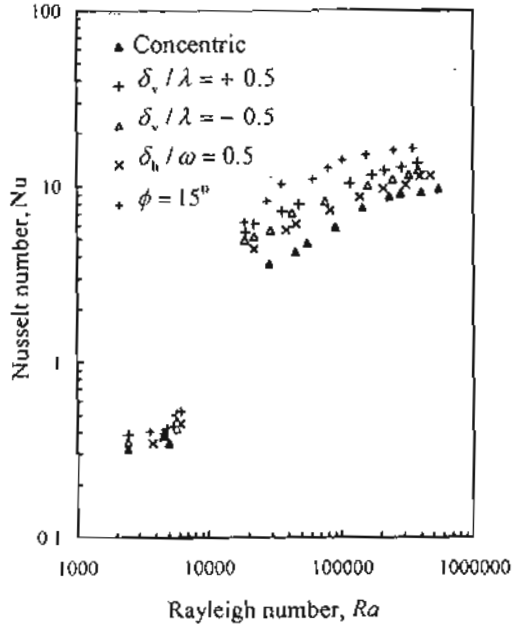

Figure (18), Nusselt number versus Rayleigh number for the pair 3 in different orientations for slender situation.

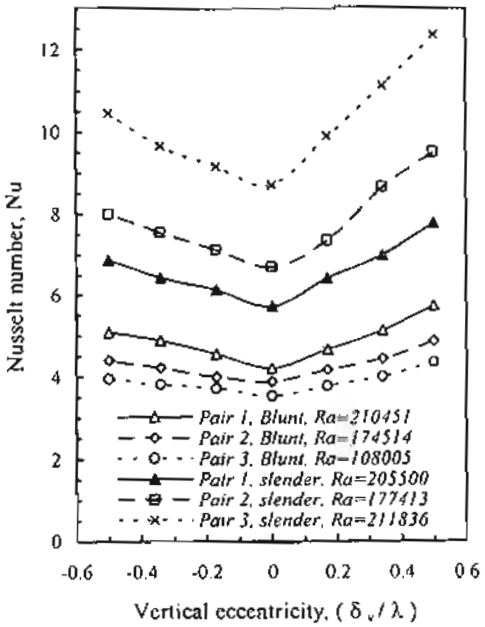

Figure (19), Effect of vertical eccentricity on the enhancement of natural convection from the three tested pairs in blunt and slender situations.

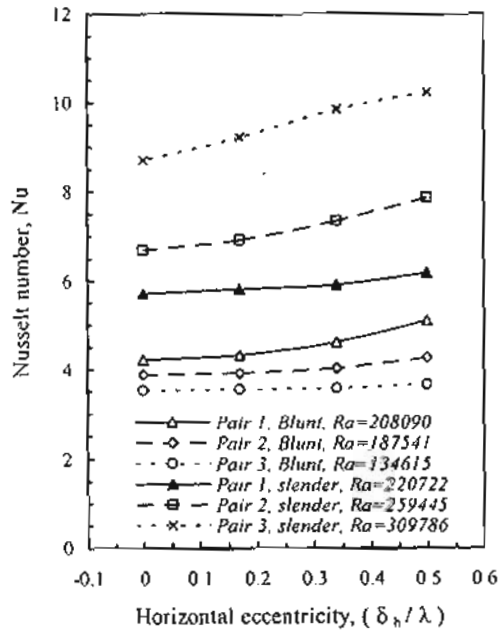

Figure (20), Effect of horizontal eccentricity on the enhancement of natural convection from the three tested pairs in blunt and slender situations.

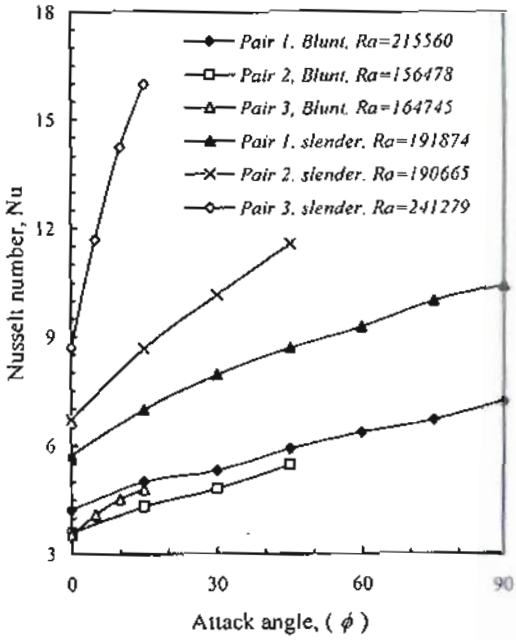

Figure (21), Effect of the attack angle on the enhancement of natural convection from the three tested pairs in blunt and slender situations.

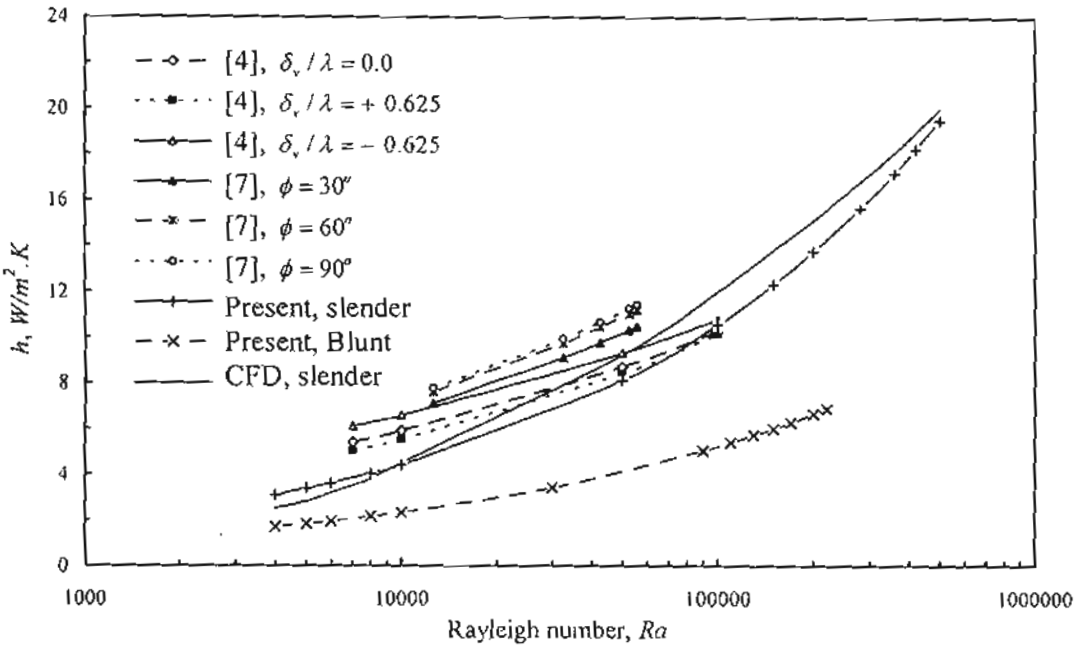

Figure (22), Comparison between present and previous works.